HIGH POWER CO LASER

V. G. Draggoo, et al

Northrop Research and Technology Center

Prepared for:

Office of Naval Research
Advanced Research Projects Agency

November 1974

UNCLASSIFIED

SECURITY CLASSIFICATION OF THIS PAGE *(When Data Entered)*

REPORT DOCUMENTATION PAGE		READ INSTRUCTIONS BEFORE COMPLETING FORM
1. REPORT NUMBER NRTC 74-56R	2. GOVT ACCESSION NO.	3. RECIPIENT'S CATALOG NUMBER AD/A-002223
4. TITLE *(and Subtitle)* High Power CO Laser Quarterly Technical Report (U)		5. TYPE OF REPORT & PERIOD COVERED Technical Report 1 June- 31 September 1974
		6. PERFORMING ORG. REPORT NUMBER NRTC 74-56R
7. AUTHOR(s) V. G. Draggoo, W. B. Lacina, and G. L. McAllister		8. CONTRACT OR GRANT NUMBER(s) N00014-72-C-0043
9. PERFORMING ORGANIZATION NAME AND ADDRESS Northrop Research & Technology Center 3401 West Broadway Hawthorne, California 90250		10. PROGRAM ELEMENT, PROJECT, TASK AREA & WORK UNIT NUMBERS ARPA Order No. 1806
11. CONTROLLING OFFICE NAME AND ADDRESS Advanced Research Projects Agency 1400 Wilson Blvd. Arlington, Virginia		12. REPORT DATE November 1974 13. NUMBER OF PAGES 44
14. MONITORING AGENCY NAME & ADDRESS *(if different from Controlling Office)* Office of Naval Research Department of the Navy Arlington, Virginia 22217		15. SECURITY CLASS. *(of this report)* Unclassified 15a. DECLASSIFICATION/DOWNGRADING SCHEDULE

16. DISTRIBUTION STATEMENT *(of this Report)*

17. DISTRIBUTION STATEMENT *(of the abstract entered in Block 20, if different from Report)*

18. SUPPLEMENTARY NOTES

19. KEY WORDS *(Continue on reverse side if necessary and identify by block number)*

CO Laser	Molecular Kinetics	Line Selection
Molecular Laser	Resonance Selfabsorption	
Electric Discharge Laser	Rotational Cross Relaxation	
High Power Laser	Heating Rate Measurement	

20. ABSTRACT *(Continue on reverse side if necessary and identify by block number)*

Effort on the High Power CO Laser Program is reviewed. The program is directed toward the development of the required CO laser technology, the required component technology, and the design and construction of intermediate power laser devices. The results of analytical and experimental investigation of the basic characteristics of the laser and data from a high pressure electrically excited CO laser device are discussed.

DD FORM 1 JAN 73 1473 EDITION OF 1 NOV 65 IS OBSOLETE

UNCLASSIFIED

SECURITY CLASSIFICATION OF THIS PAGE *(When Data Entered)*

NRTC 74-56R

HIGH POWER CO LASER
QUARTERLY TECHNICAL REPORT

Period Covering: 1 June - 31 September 1974

November 1974

Prepared by

V. G. Draggoo, W. B. Lacina, and G. L. McAllister

Contract N00014-72-C-0043

Sponsored by

ADVANCED RESEARCH PROJECTS AGENCY
ARPA Order No. 1807

Monitored by

OFFICE OF NAVAL RESEARCH
Code 421

NORTHROP CORPORATION
Northrop Research and Technology Center
High Power Laser Program Office
3401 West Broadway
Hawthorne, California 90250
(213)675-4611 Ext. 2821

PROGRAM IDENTIFICATION

ARPA Order No.:	1807
Program Code No.:	3E90
Name of Contractor:	Northrop Corporation
Effective Date of Contract:	30 September 1974
Amount of Contract:	$3,650,663
Contract No.:	N00014-72-C-0043
Program Manager	Dr. D. K. Rice (213)675-4411, Ext. 5163
Scientific Officer:	Director, Physics Program Physical Sciences Division Office of Naval Research Department of the Navy 800 North Quincy Arlington, Virginia 22217

Disclaimer: The views and conclusions contained in this document are those of the authors and should not be interpreted as necessarily representing the official policies, either expressed or implied, of the Advanced Research Projects Agency or the U. S. Government.

TABLE OF CONTENTS

1.0 INTRODUCTION

During this reporting period, modifications to the filamentary e-gun were implemented. These modifications were designed to overcome the output instabilities of the gun which occur at high filament currents. This enhanced e-gun performance was anticipated to yield greater electrical pumping of the laser thereby achieving low V-band operation. The new operating characteristics of the e-gun were improved by a factor of two yielding total gun currents of 140 amps.

Spectral line selection studies were continued during this period. Detailed quantative spectra were obtained using a Laser Precision Pyroelectric Array with an Optics Engineering CO Spectrum Analyzer. This approach contrasts the previous technique of using the ultraviolet-excited fluorescent screen to assess the strength of the laser signal. This technique allows quantitative determination of the entire spectral profile of the laser output.

Rotational cross-relaxation experiments utilizing the 10-liter device were also conducted during this period. The experimental technique was to observe the temporal development of the laser pulse for two neighboring rotational lines within a given vibrational band. The presence or absence of simultaneous lasing of the lines indicates the effect of cross-relaxation between rotational states.

A theoretical analysis of the acoustic disturbances due to laser gas heating has been accomplished. The data obtained from interferometric measurements of the laser medium and acoustic velocity measurements established the fraction of laser pump energy responsible for bulk heating of the gas. Typical values of 10% to 20% were measured for various gas mixes. These values correlate well with those predicted by the kinetic model, i.e. heating due to the anharmonic defect between V-V collision partners.

Finally, the concepts of resonance self-absorption was examined theoretically. Resonance self-absorption from overlapping lines of a CO laser medium may be an important pressure-dependent mechanism for theoretical analysis, with possible impact on line selection and atmospheric propagation. Certain presently unexplained discrepancies relating to transient time scale, spectral anomalies, efficiency degradation, and sensitivity to temperature might all be consistently resolved by this hypothesis. The developments reported here are presented in the form of the publication by W. B. Lacina and G. L. McAllister submitted to Applied Physics Letters.

2.0 E-BEAM GUN MODIFICATIONS

The e-gun modification performed during this period consisted of altering the electrical configuration of the gun filaments from series-parallel to a parallel arrangement. This results in a lower filament voltage for an equivalent filament power. The high filament voltages of the series-parallel configuration resulted in gun instabilities which limited the maximum usable output. In conjunction with this new configuration, a 10/1 transformer was added to meet the low voltage/high current filament requirements which could not be achieved with the filament high voltage isolation transformer alone. The stable gun output achieved as a result of the alteration obviates the need for the oscillation suppression electronics which were subsequently removed.

Prior to the modifications, the gun was operated with a defective filament isolation transformer. The partially shorted secondary did not limit operation of the laser at the lower power levels. Following the gun modifications it was necessary to replace the secondary in order to operate at full filament capacity. Damage to the filament transformer has been attributed to high voltage transients. Shorting capacitors have been installed to protect transformer secondary.

The e-gun modification was required in order to obtain high gun currents (>100 amp). The higher gun current yields greater ionization in the gas discharge thereby achieving larger sustainer currents. Typical maximums for the laser pumping characteristics for the pre and post e-beam gun modifications are 10-15 MW/liter-atm and 50-70 MW/liter-atm, respectively.

3.0 LINE SELECTION

During this reporting period, further line selection studies were undertaken to extend the results reported earlier.[1] In particular, emphasis was placed on obtaining low V-band output and and on observing the effect of increased electrical pumping on the spectral profile of the laser output. The enhanced output of the e-gun provided an increase in the pump rate by about a factor of five. Detailed spectra were obtained by using the scanning 64 element linear, pyroelectric array detector and a CO spectrum analyzer. The Optical Engineering CO Spectrum Analyzer normally uses an ultraviolet-excited fluorescent screen to detect the laser signal. The fluorescent detection technique is useful in identifying the laser spectral lines, but in assessing the relative strengths of the individual lines a more quantative detection technique is required. We have adapted the Laser Precision Pyroelectric Array to the CO Spectrum Ananlyzer to obtain quantative data. Figure 3.1 shows the experimental configuration for these experiments. The laser radiation is reflected off of a 45^{o} aluminum plate through the entrance slits of the spectrum analyzer. The dispersed spectrum is imaged on a plane just inside the front panel of the spectrum analyzer while the pyroanalyzer array is positioned approximately 3-4 cm beyond this plane resulting in a defocused image on the pyroelectric array. The individual spectral components are thus spread over 5 to 6 pyroelectric elements. The spread is not so large as to overlap adjacent rotational spectral components onto common pyroelectric elements. Figure 3.2 shows an oscilloscope photograph of typical experimental data. Since the pyroelectric array is 7.1 cm in length and the laser spectrum of the CO spectrum analyzer subtends a length of approximately 11 cm, two scans each with a different array position must be made to obtain the entire spectrum. This technique offers for the first time a quantitative measure of the total energy in each V-band.

Figure 3.3.a, 3.3.b, and 3.3.c are composite spectra of the CO EDL with stable optics at 72% coupling at three pump rates showing the fraction of laser energy in each V-band. The gas mix was 15/1 : N_2/CO at a total

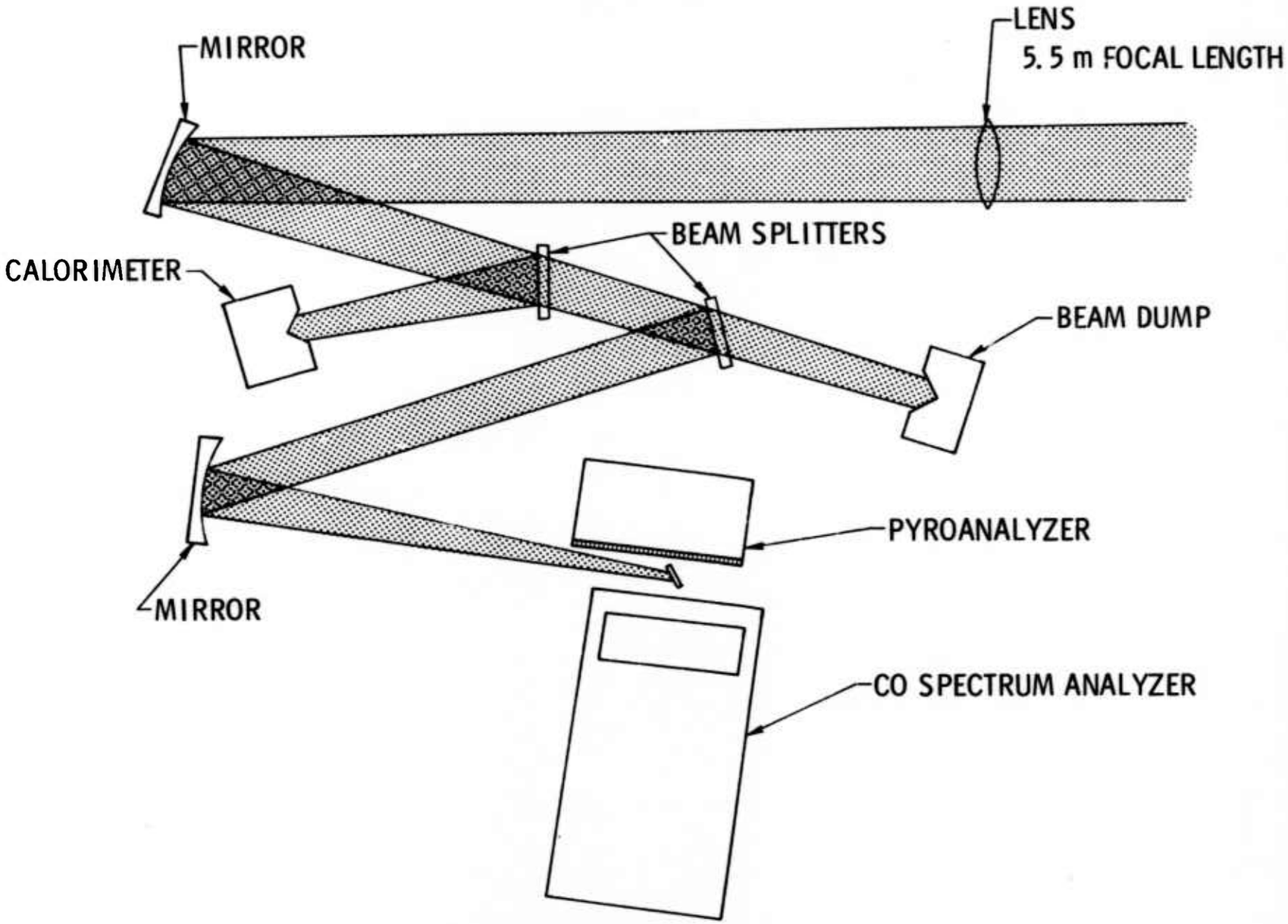

Figure 3.1. Line Selection Experimental Configuration.

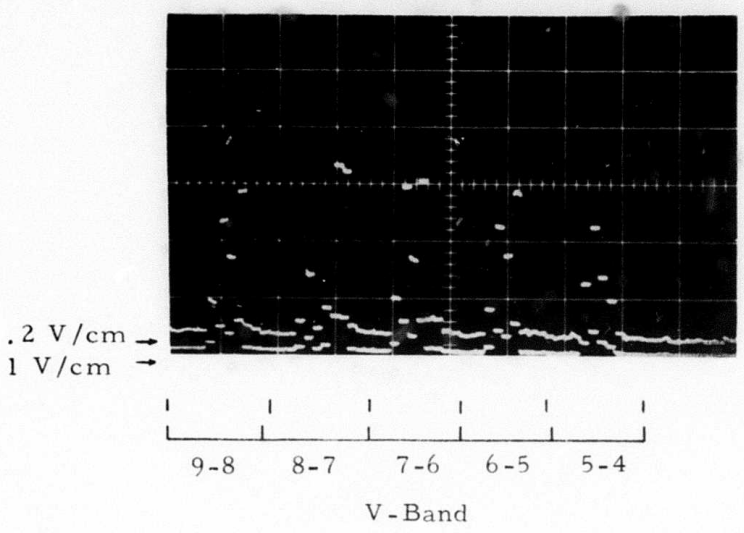

Figure 3.2. Pyroanalyzer output illustrates total energy in each V-band.

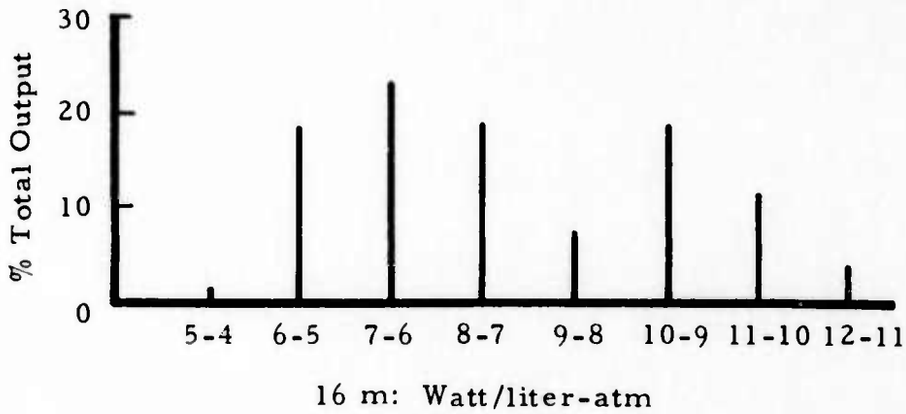

16 m: Watt/liter-atm

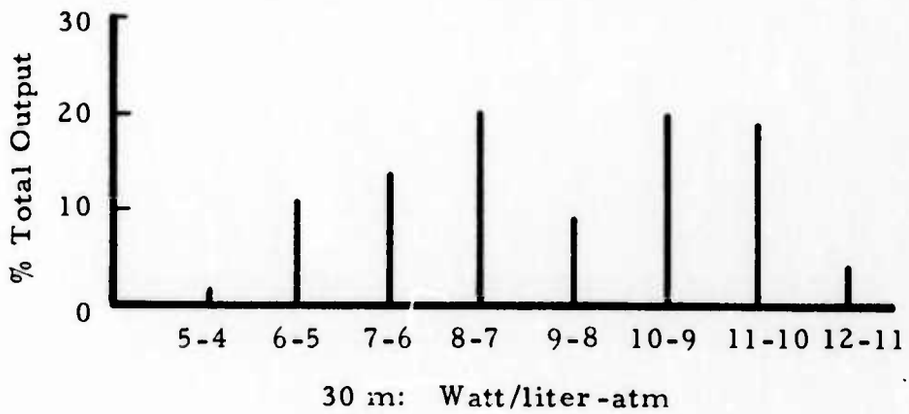

30 m: Watt/liter-atm

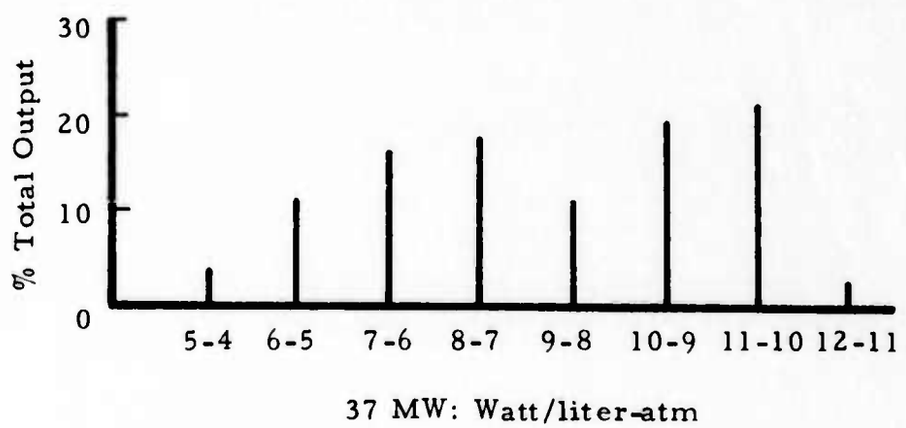

37 MW: Watt/liter-atm

Figure 3.3. Laser Output Spectra by V-Band at Three Pump Rates: Gas Mix CO/N_2 = 1/15, Total Pressure 85 Torr.

pressure of 85 Torr. Sustainer voltages were 8 kV, 10 kV and 10.5 kV. A notable feature of the spectra is the dip in energy of the 9-8 transitions. It seems unlikely that this dip is due to systematic errors of the equipment or to the experimental technique; consistent results were obtained for a variety of spectrum analyzer alignments and pyroanalyzer positions. This dip is in substantial dissagreement with the CO kinetics as they are presently understood. However, the addition of the effects of resonance self-absorption (see Appendix I) to the theoretical analysis may be important in explaining the anomolous dip at the 9-8 transition as well as the missing rotational transitions within the V-band. Another significant point is the absence of 4-3 transitions. The 4-3 transitions have not been observed with the nominal 10-liter CO EDL using 72% output coupling. Four-three (4-3) transitions have been observed in a similar CO EDL with identical output coupling and similar pumping characteristics.[2] Operating conditions for both devides were 10/1:CO/N_2 mix at 100 Torr with an electrical pump rate of 30-40 Watt/cc/Torr. An important difference between the two devices was the electric field strength; 20 V/cm/Torr for the 2 liter system and 10 V/cm/Torr for the 10 liter system. This factor of two difference in E/P may have a substantial effect on the spectral output.

Additional parametric studies of the 10 liter EDL output spectrum were performed. In particular, obtaining 4-3 transitions was the principle goal. The similar pumping characteristics of the 2 liter device suggests that the 10 liter device is operating near the 4-3 threshold. Output coupling experiments were performed to achieve oscillation of the 4-3 band. Figure 3.4 are photographs of the ultraviolet excited fluorescent screen of the spectrum analyzer. This spectrum was obtained using a 60% reflecting resonator mirror. The pump rate was 40 W/cc/Torr with 15/1:N_2/CO mix at 85 Torr. Four-three (4-3) transitions at 2008 cm^{-1}, 2012 cm^{-1} and 2020 cm^{-1} are identified as 4-3 P(14), 4-3 P(13) and 4-3 P(11). Under

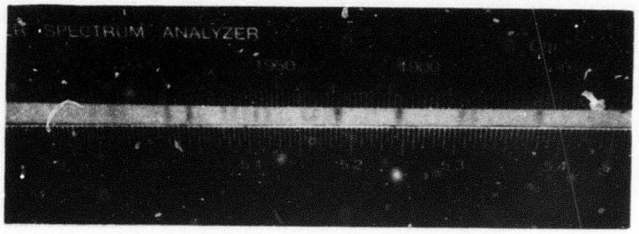

a. $P(H_2O)$ = 0 Torr

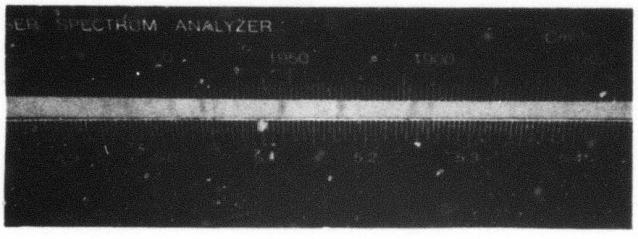

b. $P(H_2O)$ = 600 Torr @ 155°C

P_T = 85 Torr

N_2/cc = 15/1

W_{in} = 2.5 kW/cc (ΔT = 60 μsec)

T = 80°K

Figure 3.4. Output spectra of nominal 10-liter CO EDL with and without line selection.

these operating conditions, spectral line selection experiments employing the water vapor cell previously described[3] were also performed. Comparison spectra are shown in Figure 3.5.a and 3.5.b for 0 Torr H_2O vapor and 600 Torr H_2O vapor. The value listed above each spectral line is the predicted e-folding distance for the Midlatitude Winter Atmospheric Model at sea level.[4] The height of each line is a qualitative representation of its relative intensity as interpreted from photographic data illustrated in Figure 3.6. Here as was shown in previous experiments,[3] many lines of relatively low e-folding distances are absent due to absorption by the intracavity cell and in the case of the 5-4 and 9-8 transitions new lines appear at 5-4 P(11) and 9-8 P(9).

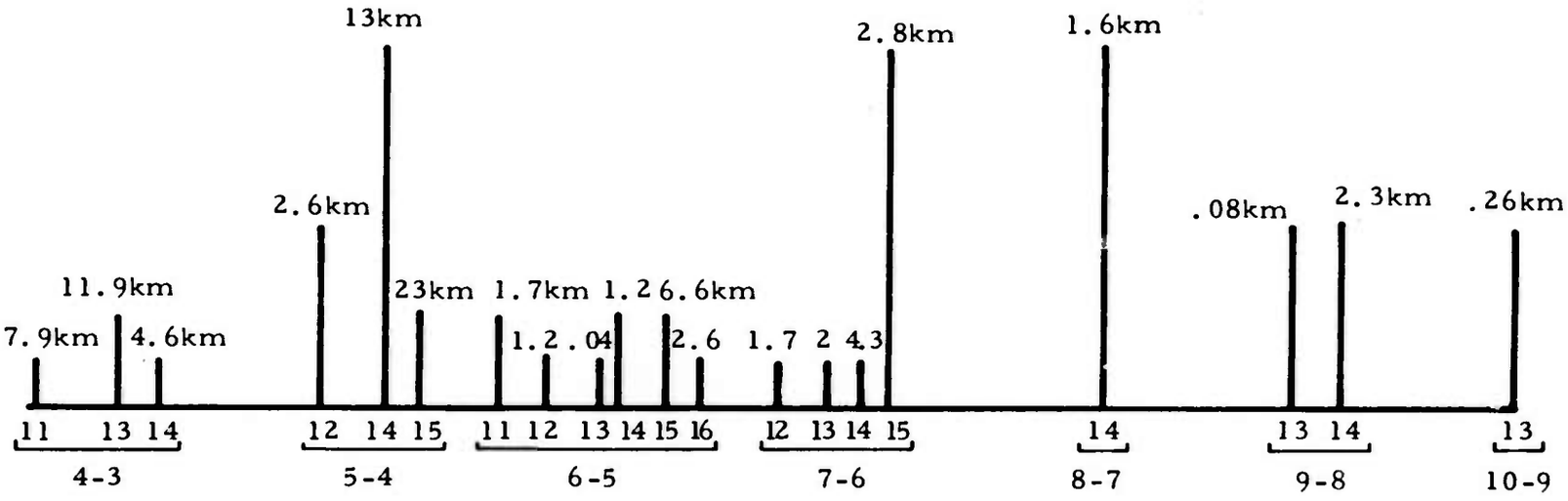

a) $P(H_2O)$ = 0 Torr

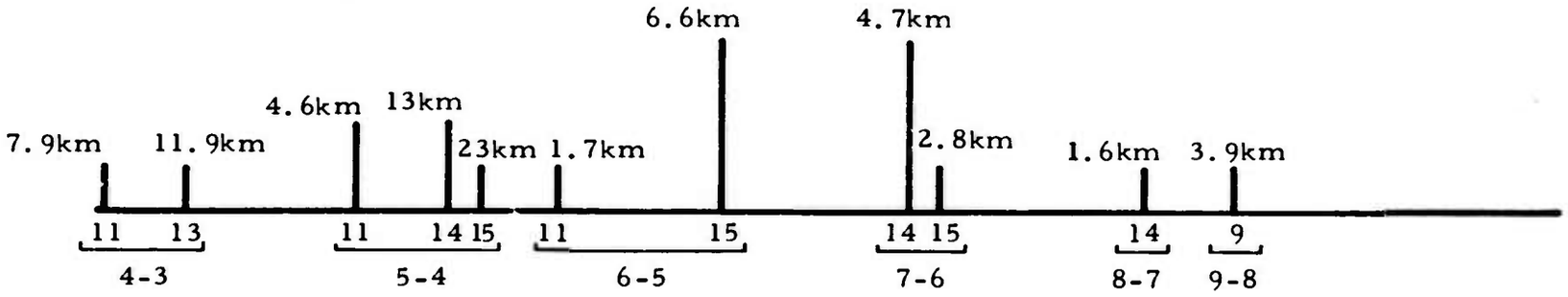

b) $P(H_2O)$ = 600 Torr @ 155°C

P_T	= 85 Torr
N_2:CO	= 15:1
W_{in} 3.4	= kW/cc (Δt = 80 μs)
T	= 80°K
4090	= Optical Output Coupling

Figure 3.5. Laser Output Spectra.

4.0 ROTATIONAL CROSS-RELAXATION EXPERIMENTS

Rotational cross-relaxation rates in CO are estimated to be fast relative to V-V rates. The present kinetics code assumes a rotational temperature equal to the kinetic temperature. In this case the rate is infinite, and in the analysis of the laser performance, cascading of the radiation from V-band to V-band and distorted rotational population distributions do not occur. However, cascading is observed[5] and the effects of "burned down" rotational distributions have been discussed.[6] It is apparent from the experimental data that the effects of finite rotational cross-relaxation time constants are observed. These effects have particular importance to line selection employing an intracavity absorber; fast R-T rates are needed for efficient line selection.

A set of measurements designed to set bounds on the rotational cross-relaxation rate were performed utilizing the 10 liter EDL. The experimental technique was to observe the temporal development of the laser pulse for a pair of neighboring rotational lines within a V-band. In these experiments optical masks were placed over the output aperture of a Optics Technology CO Spectrum Analyzer such that only the 7-6 P(10) and 7-6 P(11) were allowed to pass each to a separate Ge:Au detector. If significant oscillation of both lines occurs simultaneously, then the rotational rate is of the order of the V-V pump rates. The experiment was performed using the unstable resonator with both Ar/CO and N_2/CO gas mixtures at various pressures.

Figure 4.1 contains oscilloscope photographs showing the response for a neighboring rotational pair. The gas mix and pressure was Ar/CO and 85 Torr. It is clear from the photographs that simultaneous lasing does occur. The photographs also indicate that the transitions are not oscillating independently in that as the second pulse begins the first pulse is beginning to fall. The coincidence in time between the rise of the P(11) and the fall of the P(10) indicates that the P(11) is building at the expense of the P(10), but the finite buildup time indicates the rate of rotational cross-relaxation is finite and is important for the time scales of the pulsed devices. An additional effect

7-6 P(11)

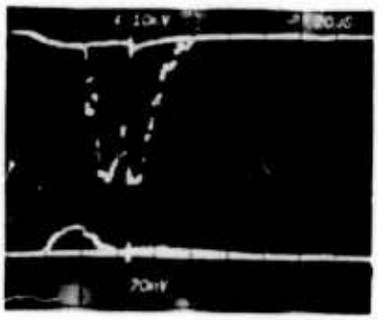

7-6 P(10)

Figure 4.1. Temporal response of two neighboring J transitions of 7-6 V transitions. Gas mix Ar/CO:6/1 at total pressure of 85 Torr.

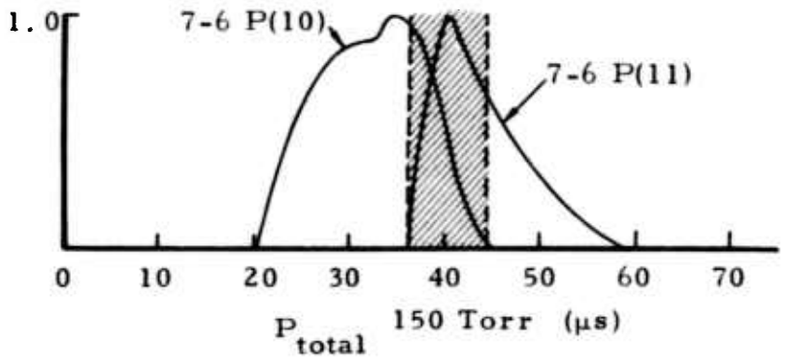

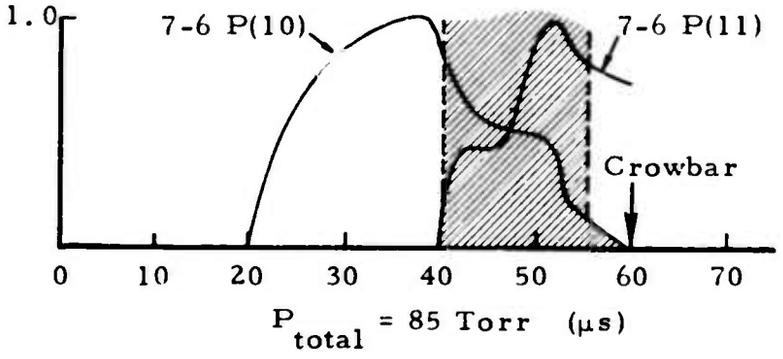

Figure 4.2. Pressure effects of rotational cross-relaxation. Cross-hatched region represents periods of simultaneous lasing.

is that of pressure. The rotational cross-relaxation mechanism is represented by the R-T process

$$CO_{N,J} + X \rightarrow CO_{N,J\pm} + X + \Delta E$$

where N is the vibrational quantum number

J is the rotational quantum number

X is any other gas constituent.

The rate is therefore a pressure dependent rate from which we would infer the rotational relaxations to be more rapid at higher pressure. Figure 4.2 contains sketches of laser pulses for pressure of 85 Torr and 100 Torr. Clearly the percent overlap of the 150 Torr case is less than that of the 85 Torr case. This is consistent with the hypothesis of the R-T process.

These experiments were intended to determine if the effect rotational relaxation could be observed. The experiments in themselves cannot assess the rates but only indicate the effect.

5.0 ACOUSTIC ANALYSIS AND BULK GAS HEATING

Electric discharge lasers in general convert a significant fraction of the electrical excitation power into heating the laser gas. Although the quantum efficiency of the CO EDL is exceptionally high[7] (>90%) and the heating rate is very low[8] (~20%), for high power operation the excitation rate is still sufficient to produce large temperature increases in the gas. If the laser gas is completely confined and the discharge uniformly fills the entire volume then the pressure increases with the temperature but no gas motion or density change occurs. The discharge region for the 10 liter device is confined on the sides and ends, but the plane at the top (cathode) is essentially free and the plane at the bottom (anode) is slightly porous. When the discharge is initiated, the gas between the cathode and anode is heated while the gas above the cathode and below the top surface of the anode is unaffected. The pressure gradients which thus appear across these boundaries force gas from the discharge region at the top and bottom and lead to rarefaction waves which propagate into the discharge. Also intense heating near the cathode (cathode fall heating) generates an additional compression wave which propagates into the medium. Interferograms of the discharge region showing the optical effects of the acoustic disturbances have appeared in a previous report.[3]

An acoustic theory has been developed to study the relationship between the heating rate and the wave amplitude and wave velocity. For the short pulse durations and small magnitudes of the acoustic disturbances considered here, the gas conditions can be described by the following equations:

$$\partial \rho / \partial t + \rho_o \nabla \cdot \bar{v} = 0 \qquad (1)$$

$$\rho_o (\partial \bar{v} / \partial t) + \nabla p = 0 \qquad (2)$$

$$dU_i/dt + p_o \nabla \cdot \bar{v} = \dot{Q} \tag{3}$$

$$p_o = \rho_o RT \tag{4}$$

where
- ρ = density change
- p = pressure change
- $\bar{v}$ = velocity change
- T = temperature
- $U_i = C_v T$ (Joule/cm^3)
- $\dot{Q}$ = heat addition (W/cm^3)
- R = gas constant (Joule/^{o}K/gm)

These equations are, respectively, the continuity equation, conservation of momentum, conservation of energy and the equation of state. The zero subscription implies the unperturbed conditions. For spatial variations only in the y;direction, the wave equation for the pressure variations is

$$\partial^2 p(y,t)/\partial y^2 - [1/c_o^2]\, \partial^2 p(y,t)/\partial t^2 = [-(\gamma - 1)/c_o^2]\, \partial \dot{Q}/\partial t \tag{5}$$

where $\gamma = C_p/C_v$ and c_o is the acoustic velocity prior to the disturbance. If we consider only the wave at the cathode and follow Culick, et al,[9] then, under assumptions that 1) no reflections occur, 2) the cathode is completely porous and is not heat conducting and 3) the bulk heat deposition, Q_b, and the cathode fall heat deposition, Q_c, are uniform then

$$\begin{aligned} p(y,t)/p_o = [(\gamma - 1)\, Q_b/p_o] \{ & t - 1/2(t - y/c_o)\, H[t - y/c_o] \\ & + [\dot{Q}_b/\dot{Q}_c]\, (1/2[t - (y-d)/c_o]\, H[t - (y-d)/c_o] \\ & - 1/2[t - t_p - (y-d)/c_o]\, H[t - t_p - (y-d)/c_o] \\ & + 1/2\, [t - y/c_o]\, H[t - y/c_o] - 1/2[t - t_p - y/c_o] H[t - t_p - Y/c_o]) \} \end{aligned} \tag{6}$$

where d = width of cathode fall

t_p = electrical excitation time

$H(t, y)$ = step function

A similar wave propagates from the anode, but due to the relatively high acoustic impedance of the anode screen and the weak anode fall, this wave is somewhat weaker. Finally, the density is related to Equation (6), the expression

$$\rho/\rho_o = [1/\gamma][p/p_o - \Delta E_{in}/U_i] \tag{7}$$

where E_{in} = heat input (J/cm^3)

The result is a density wave which propagates from the cathode (and a smaller one from the anode) into the discharge region with the general appearance shown in Figure 5.1. Physically, the abrupt change is due to the heating in the cathode fall region and the linear slope behind this is produced by bulk heating of the gas. The slope of this density change is proportional to the heating rate. At the end of the electrical excitation pulse the heating terminates in the cathode fall region but the bulk heating continues for some time. Thus there is another abrupt change in the density, but the linear slope remains approximately constant.

The fact that the heating rate is proportional to the density gradient can be seen by differentiating Equation (6) and Equation (7) to obtain

$$\frac{d(\rho/\rho_o)}{dx} = \frac{(\gamma - 1)}{2\gamma} \frac{\dot{Q}b}{c_o p_o} \tag{8}$$

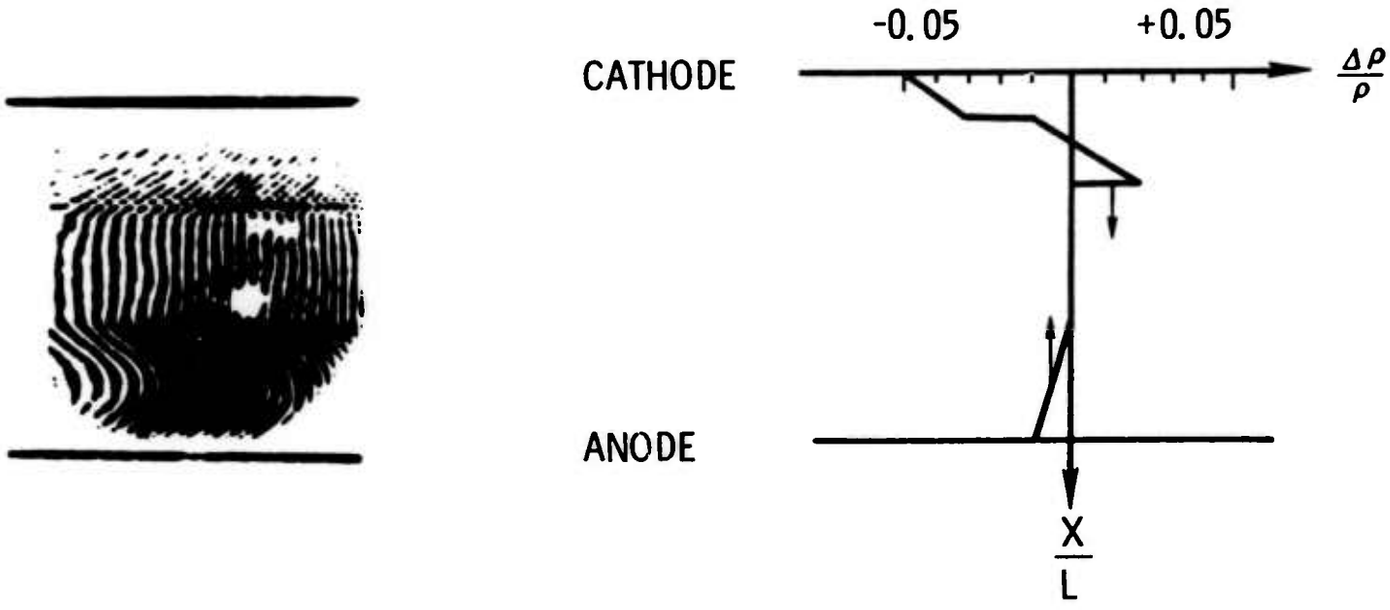

Figure 5.1. Experimental and Theoretical Density Variations Produced by Cathode and Anode Waves.

By defining the heating rate (η) as the fraction of electrical pump excitation that goes into heat we can obtain an expression for heating rate.

$$\eta = Q_b/E_{in} = [2\gamma/(\gamma-1)](c_o p_o/E_{in})[d(\rho/\rho_o)/dx] \qquad (9)$$

The density gradients can be measured from the interferograms and are plotted in Figure 5.2 against the input power for various gas mistures and sustainer voltages. η may thus be calculated from Equation (9) and plotted versus E_{in} in Figure 5.3 for various gas mixtures and sustainer voltages. The following observations may be drawn from Figure 5.3. The heating rate calculated from the density gradient analysis lies between 8% and 20% and is consistent with heating rates calculated from CO laser kinetics.

An alternative method of obtaining the laser gas heating has been deveioped using the temperature dependent velocity of propagation for the acoustic disturbances. Figure 5.4 shows interferograms of the discharge region for two electrical excitation rates. The pulsed ruby interferogram were taken 180 μsec after the initiation of the 70μsec electrical excitation pulse. Note that the wavefront of the acoustic wave has propagated further into the discharge region for the 4.5 W/cc/Torr excitation case than for the 1.6 W/cc/Torr case thus indicating a greater temperature rise for the higher excitation rate. The velocity of propagation for acoustic waves is

$$v = \sqrt{\gamma p/\rho} \qquad (10)$$

where $\gamma = C_p/C_u$

Using the equation of state (Equation 4) the velocity can be written as

$$v(t) = \sqrt{\gamma(\gamma-1)\, RT(t)/m}$$

$$= \sqrt{\gamma(\gamma-1)}\ (U_i + \eta\, W_e\, t)^{1/2} \qquad (11)$$

where W_e = electrical excitation rate (W/cc)

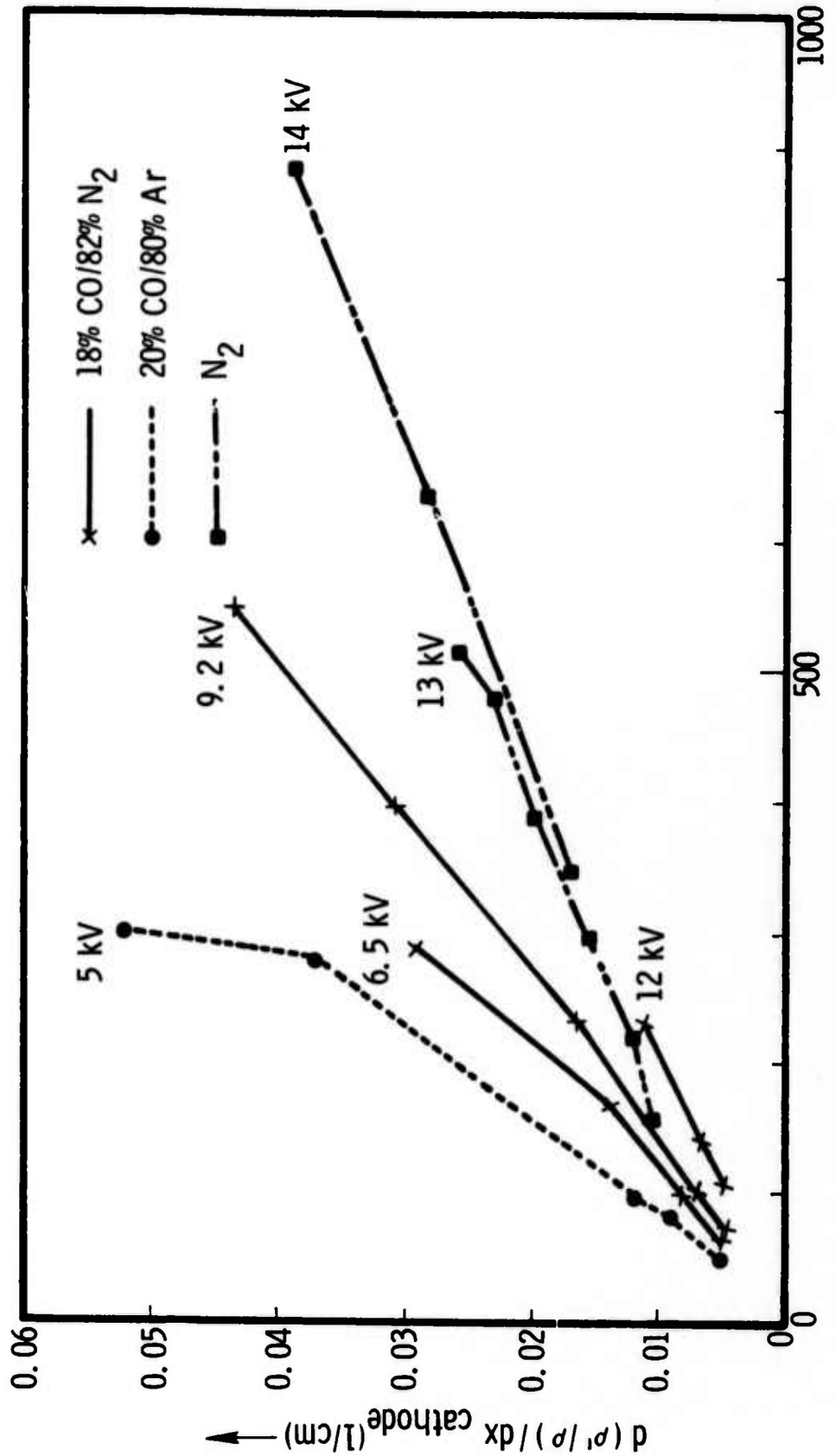

Figure 5.2. Density gradient versus pump rate.

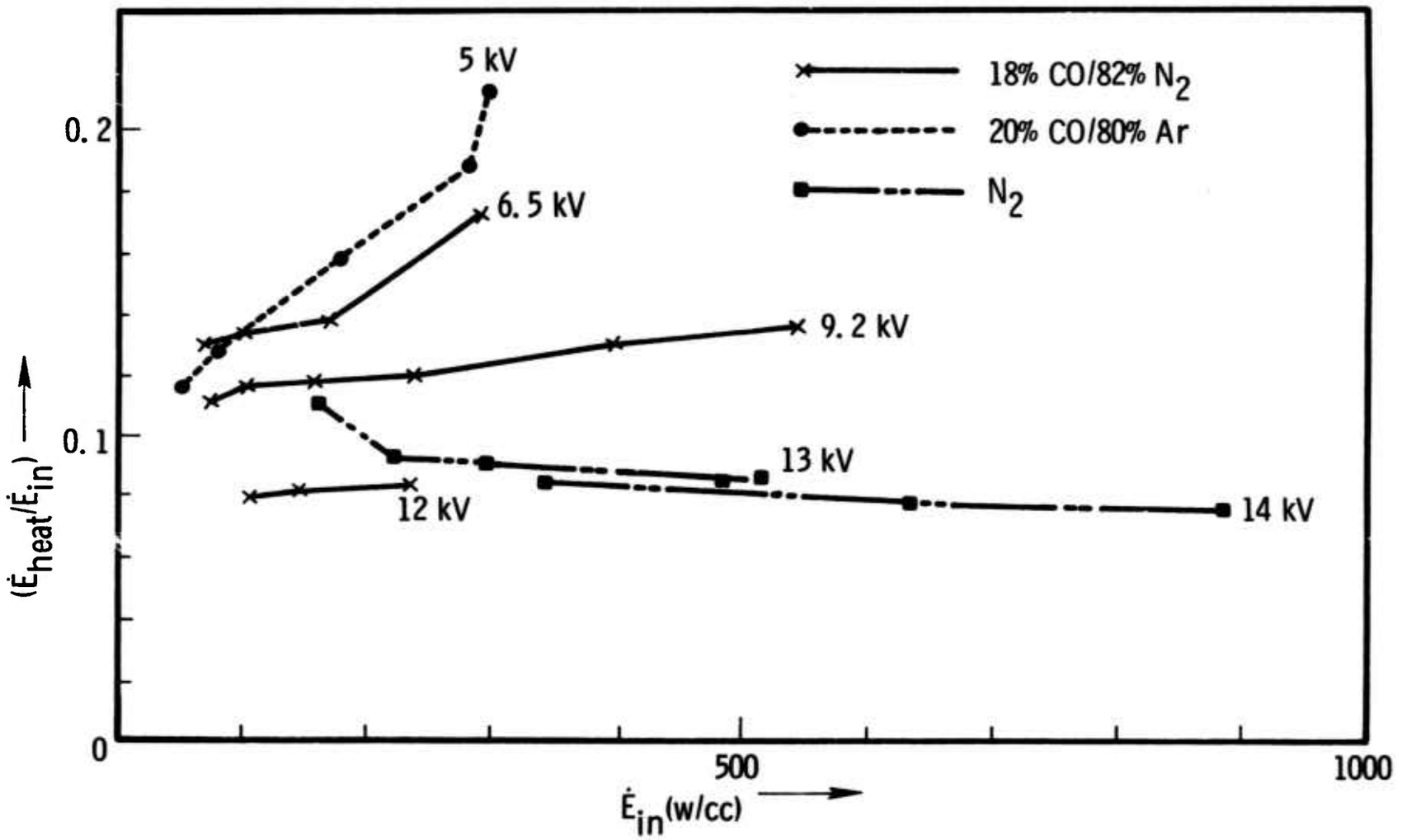

Figure 5.3. Fractional heating rate versus pump rate.

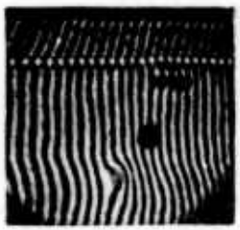

GAS MIX N_2/CO 6/1
PUMP RATE 1.6 Watt/cc-Torr

GAS MIX N_2/CO 6/1
PUMP RATE 4.5 Watt/cc-Torr

Figure 5.4. Interferograms of laser discharge showing effect of pump rate on velocity of propagation of acoustic waves.

Integrating this equation the distance of propagation can be found for any time, and conversely, the time of propagation through a given distance may also be calculated. These calculated values can then be compared with the experimentally measured acoustic velocities.

In addition to interferometric data on the acoustic disturbances, we have observed perturbations of the laser output due to the transit of the acoustic waves through the optical origin of the unstable resonator of the laser. Figure 5.5 is a schematic diagram of the output aperture of the laser which illustrates the propagation of the acoustic waves across the laser volume. The position of the central output coupling mirror and the large aperture mask are shown in relation to the density disturbances (crosshatched) which are closing from the top and bottom. As the waves propagate through the resonator axis (center of small mirror) a slight increase in laser output occurs. The physics of the output perturbations are unclear. We base our argument on the coincidence in time of the "glitches" with the predicted acoustic wave transit of the resonator origin. Certainly it is not unreasonable that the compressional component of the acoustic wave may be responsible for slight heating of the gas hence a perturbation in the optical gain. When the perturbation occurs at the resonator origin, it is subsequently amplified as it passes through the resonator. Figure 5.6 are oscilloscope photographs of the temporal laser pulse for two excitation rates. The output perturbation for the 25 W/cc/Torr occurs at 158 μsec while for the 16 W/cc/Torr case the perturbation occurs at 176 μsec. Actually two "glitches" in the laser pulse occur because the resonator axis is not precisely positioned midway between anode and cathode hence the acoustic disturbances from the top and bottom arrive at slightly different times. Figure 5.7 is a plot of acoustic transit time to the resonator axis versus pump rate for three fractional heating rates: $\eta = 0.1$, 0.2 and 0.3. Experimental times for the "glitches" are also plotted for various pump rates. These data indicate a heating of 20% and is consistent with the heating calculated from measurement of the density gradient observed in the interferometric data.

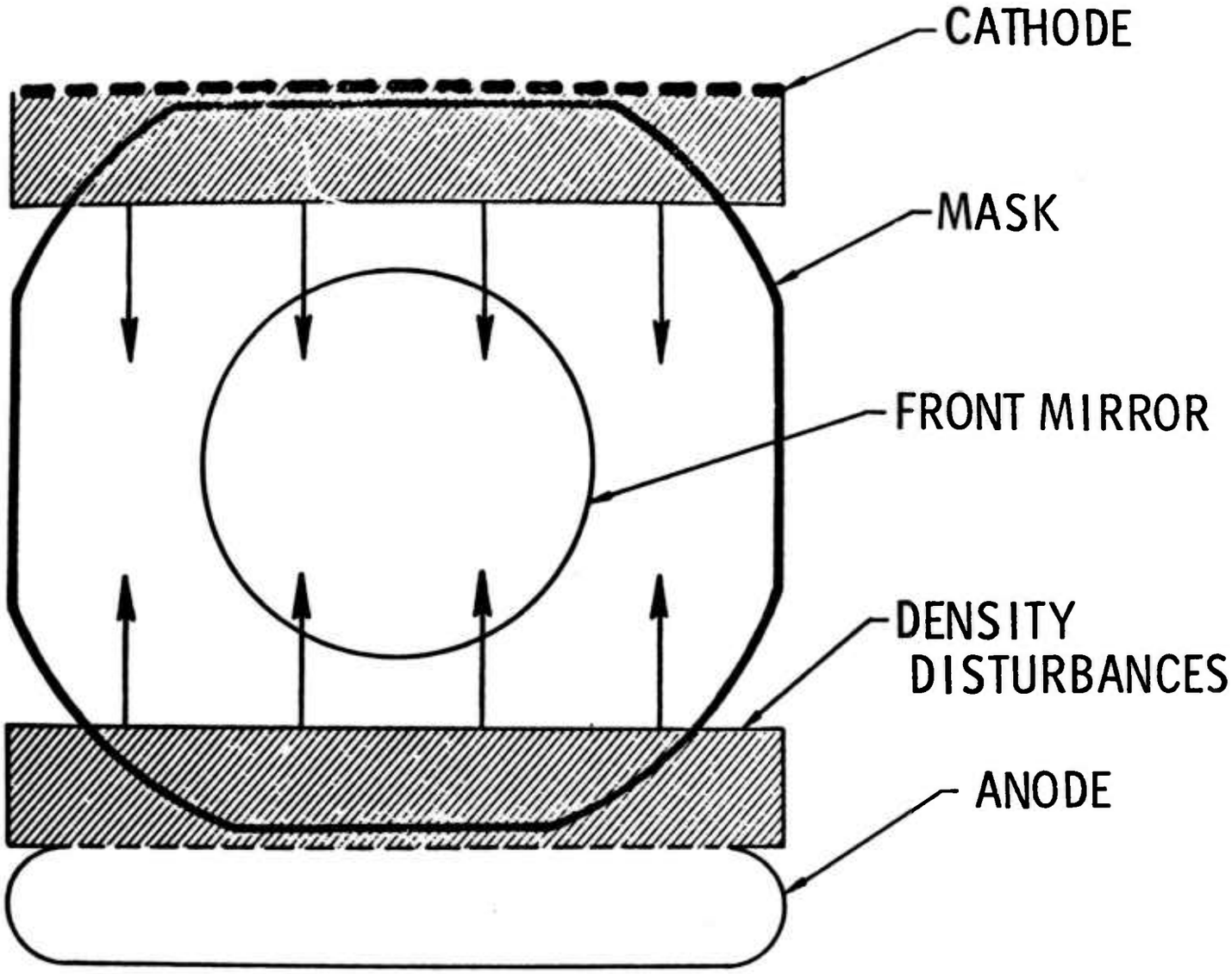

Figure 5.5. Laser cavity configuration illustrating the density disturbances and the aperturing mask.

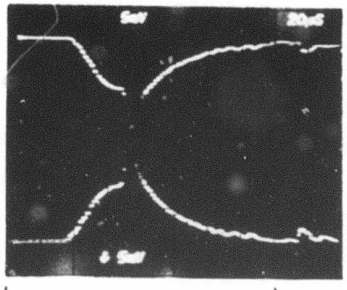

176 μs

GAS MIX: N_2/CO–6/1
TRANSIT TIME: 176 μsec
PUMP RATE: 15 Watt/cc-Torr

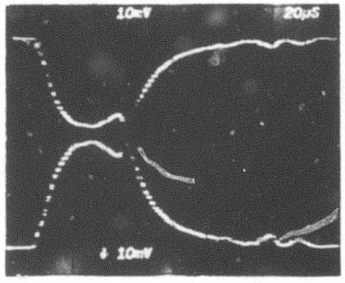

158 μs

GAS MIX: N_2/CO–6/1
TRANSIT TIME: 158 μsec
PUMP RATE: 25 Watt/cc-Torr

Figure 5.6. Laser pulse (lawn trace) with output perturbations versus pump rate.

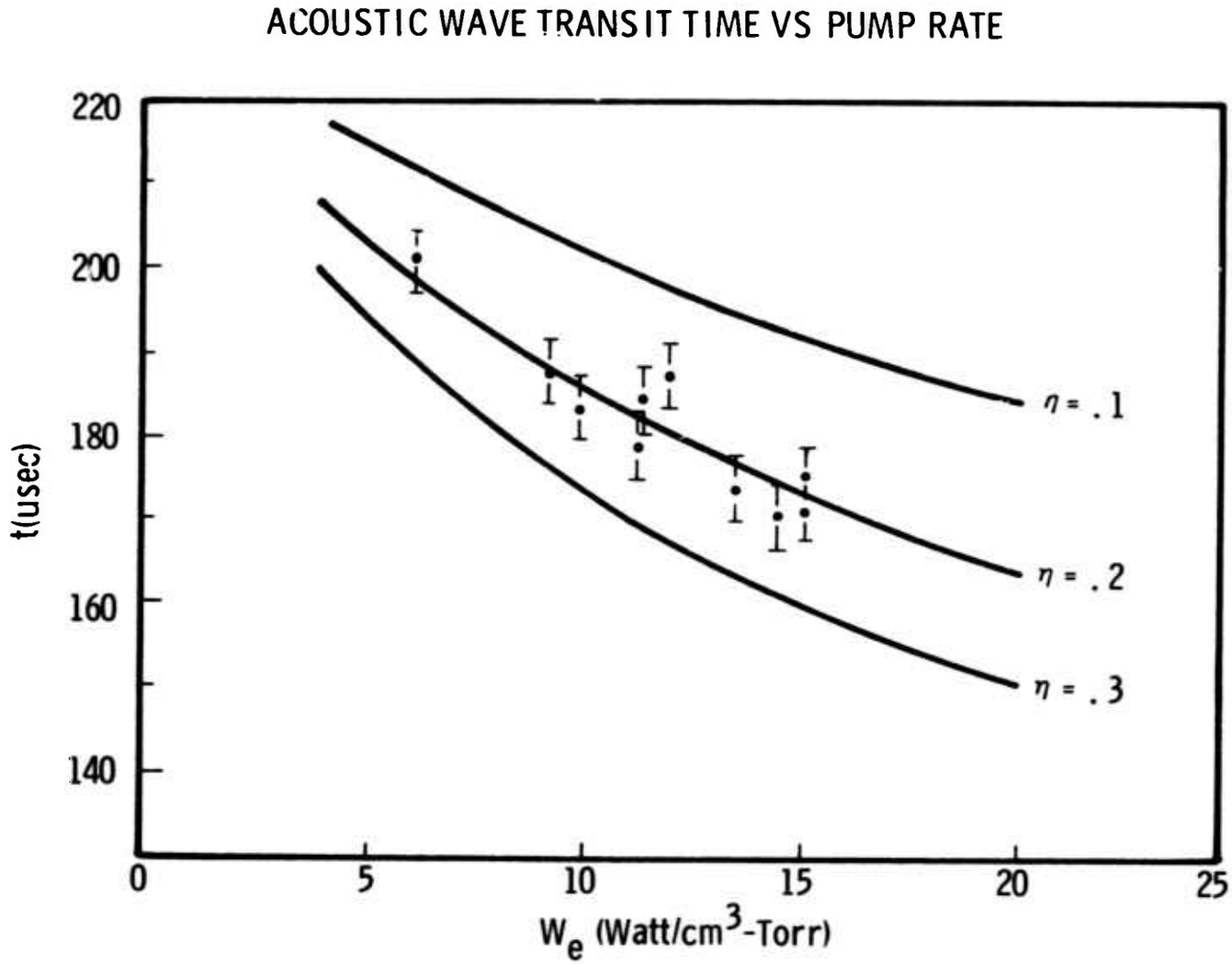

Figure 5.7. Acoustic wave transit time versus pump rate.

6.0 REFERENCES

1. G. L. McAllister, D. K. Rice, and V. G. Draggoo, "High Power CO Laser Quarterly Technical Report," NRTC 74-33R, (July 1974).

2. W. B. Lacina, V. G. Draggoo, M. L. Bhaumik, G. L. McAllister, D. K. Rice and M. M. Mann, "High Power CO Laser Sixth Quarterly and Semiannual Technical Report," NRTC 73-38R, (November 1973).

3. G. L. McAllister, W. B. Lacina, D. K. Rice and P. J. Mendoza, "High Power CO Laser Semiannual Technical Report," NRTC 74-21R, (May 1974).

4. D. K. Rice, "Carbon Monoxide Spectral Line Selection Studies," AD 749-823 (August 1972).

5. C. K. N. Patel, "Vibrational-Rotational Laser Action in Carbon Monoxide," Phys. Rev., Vol. 141, No. 1, (January 1966).

6. W. B. Lacina, G. L. McAllister and V. G. Draggoo, "High Power CO Laser Quarterly Report," NRTC 74-10R, (January 1974).

7. M. L. Bhaumik, W. B. Lacina, and M. M. Mann, "Characteristics of a CO Laser," IEEE Journal of Quantum Electronics, Vol. 9E-8, No. 2, (February 1972).

8. R. G. Eguchi, G. L. McAllister, and V. G. Draggoo, "Acoustic Velocity Measurements to Determine Laser Gas Heating Rate," presented at 27th Gaseous Electronics Conference, Houston, Texas, (22 October 1974).

9. F. E. C. Culick, P. I. Chen, and W. S. Griffin, "Studies of Acoustic Waves Formed in an Electric Discharge CO Laser Cavity," to be published.

7.0 APPENDIX

Resonance Self-Absorption in CO Lasers*

W. B. Lacina and G. L. McAllister
Northrop Research and Technology Center
Laser Technology Laboratories
Hawthorne, California 90250

ABSTRACT

Resonance self-absorption from overlapping lines in a CO laser medium may be an important pressure-dependent mechanism for theoretical analysis, with possible impact on line selection and atmospheric propagation. Certain presently unexplained discrepancies relating to transient time scale, spectral anomalies, efficiency degradation, and sensitivity to temperature might all be consistently resolved by this hypothesis.

*Research supported in part by the Advanced Research Projects Agency of the Department of Defense and monitored by the Office of Naval Research under Contract N00014-72-C-0043.

High optical extraction efficiencies for CO electric discharge lasers have been theoretically predicted and experimentally demonstrated.[1,2] The theoretical predictions are based on laser kinetic models that make several important assumptions, many of which are necessarily approximations, while others may be omissions. In general, results of calculations have agreed reasonably well with experimental comparisons at cryogenic temperatures[3,4], although there remain several other theoretical discrepancies which need to be resolved. In this regard, we wish to propose the hypothesis that resonance self-absorption in the CO medium itself may be an important pressure-dependent effect, with consequences for correct theoretical modelling of the laser, as well as possible impact on line selection and atmospheric propagation. At pressures approaching atmospheric, line broadening in the CO laser is dominated by collisions, with a half-width $\sim 0.05\text{-}0.1\ cm^{-1}$ (Doppler broadening is much less, and is important only at low temperatures, with pressures $\lesssim 20$ Torr.) Therefore, at high pressures, the collision broadening of lines results in several significant overlaps for almost every CO transition; Fig. 1 illustrates a Lorentzian gain line centered at a frequency ν_o with a nearby resonant absorption line shifted by a collision half-width $\Delta\nu$. Table I summarizes several overlaps, along with their frequency separations, for several lines which are of interest because of their favorable atmospheric transmission characteristics. It will be shown in the present discussion how such a hypothesis can have important pressure-dependent consequences, and that certain presently unexplained discrepancies relating to transient time scale, spectral anomalies, efficiency degradation, and sensitivity to molecular temperature might all be consistently resolved by this mechanism. An experimental and theoretical comparison of

scaling generalizations with a discussion of resonance absorption has been presented recently.[5]

All contemporary theoretical models of CO laser kinetics have overlooked the fact that laser oscillation on one vibrational-rotational band could be absorbed (or have enhanced gain) by near resonant transitions of other bands. However, at high pressures ($\gtrsim$100 Torr), collision broadening of lines begins to result in several significant overlaps. Of particular importance is the fact that the P(J) transitions (which are the ones which oscillate) most frequently have overlaps with R(J) transitions of <u>higher</u> vibrational bands, and thus absorptive pumping to higher v-levels results. Thus, the pressure dependence predicted by current kinetic models is probably not accurate, and such models may be seriously invalid for prediction of detailed spectral distributions.

Initial calculations have been carried out using an existing kinetics code[3] for a pulsed, atmospheric pressure CO electrically excited laser at 100°K, pumped at 10 kW/cm^3 (typical of present e$^-$-beam sustained CO EDL devices), with a CO/Ar = 1/6 mixture. As the transient analysis evolved from laser threshold to steady state, all transitions which were predicted to oscillate were examined for other resonant transitions. Gains or absorptions, as well as the rate of pumping (cm^{-3}s^{-1}), were compared with those from the existing code, which does not include resonance processes. It was found that rates of absorption on overlapping bands was typically one to two orders of magnitude higher than rates originating from VV or VT kinetic or electron excitation collisions. Thus, self-absorption competes strongly with all other kinetic excitation rates, which implies that the theoretically predicted radiation intensities from such a model are probably significantly in error if resonance absorption is not included properly. A refinement

and extension of the laser kinetics code has been undertaken to properly include, in a completely self-consistent way, all of the gain and absorption processes in the CO medium to determine radiation intensities for a CO oscillator analysis. These calculations are in progress, and results will be presented in the near future.

The important consequences that are anticipated from this analysis will be described briefly here, with experimental evidence that now exists supporting this hypothesis. Results of future calculations will determine the range of parameters (primarily pressures) for which the effects would be significant.

1) Transient Time Scale

The absorption of the medium has a direct effect on the attainment of gain, and thus, it is to be expected that laser threshold time will be increased, and that transient evolution to steady state will be lengthened. Experimental data from a CO e^--beam sustained EDL (50-200 Torr at 80^oK) was compared with theoretical scaling predictions[4,5], and results showed that both threshold and steady state times were delayed from the predicted values.

2) Spectral Anomalies

Theoretical calculations predict that output spectral distributions should lie about one or two v-bands lower than what is usually observed. Furthermore, experimental output spectra often show that certain transitions are always missing: it was from this observation that the hypothesis of resonance self-absorption was first conceived to be an important mechanism. Typically, the existence of resonances will result in one of two possibilities: (a) the absorptions are so strong that laser oscillation is permanently inhibited from certain transitions; or (b) oscillation occurs, but output coupling

efficiency is degraded and higher vibrational levels are absorptively pumped. The first effect can have serious consequences for line selection, since it becomes possible that certain good atmospheric transmission lines may never be attainable from a high pressure device. For example, the $6 \rightarrow 5$, P(10) transition has never been observed from the e^--beam CO EDL even at total pressures $\sim$ 85 Torr at $100^{o}K$, with an intracavity water vapor line selection cell. (Refer to Table I.) The second possibility (b) may have serious consequences for degradation of the optical extraction efficiency, kinetic gas heating, and temperature dependence. These are discussed below.

3) Optical Extraction Efficiency

Theoretical calculations of the total optical output extraction have generally shown that quantum efficiencies usually approach a universal steady state value of $\sim$ 90%, with little dependence on molecular temperature or electrical pumping rates. It is found experimantally, however, that room temperature operation is significantly less favorable than the optimistic predictions of existing theoretical models, and quantum efficiencies of $\sim$ 90% have not yet been attained even at low temperatures. Degradation of optical extraction efficiency, as well as the poor agreement with high temperature predictions, can both be qualitatively explained by the resonance absorption hypothesis as follows. The optical extraction per unit volume is determined by a combination of quantum efficiency and output coupling efficiency, where the latter is the ratio of the output coupling loss/pass, divided by the total loss/pass. If a line has attained sufficient gain to lase, absorption in the medium is effectively added to other losses (e.g., windows) in the cavity, and thus, absorption in the medium (which is typically from R(J) transitions of higher v-bands) will result in a degraded coupling ratio. Furthermore, the absorptive pumping of the high vibrational levels will move the spectrum upward, as well as degrade the predicted

quantum efficiency, since VV heating will be increased and the capacity to extract energy in the form of laser radiation is reduced. Increased kinetic heating results when the population distribution is pumped to higher vibrational levels.

4) Temperature Dependence

At higher temperatures, for a given density, the collision broadened half width is increased, and therefore the number of resonant absorption overlaps that may contribute is increased. Furthermore, gain and absorption are strong functions of kinetic temperature, so the increased absorptive pumping of higher vibrational levels may explain the poor performance characteristics of high pressure room temperature CO lasers. Lastly, the P(J) transitions are shifted to higher J values at high temperatures, and this may result in R(J) resonances with more severe absorptive characteristics. It has often been speculated that this unexplained discrepancy in predicted temperature dependence may be due to an inadequate knowledge of the VV cross-relaxation rates. However, calculations show that this possibility cannot account for the effect, and thus, resonance self-absorption may be able to resolve the unexplained sensitivity to temperature dependence.

5) Frequency Pulling and Pushing

In general, the gain for any CO transition is a sum of Lorentzians over all of the resonant lines, as shown in Fig. 1; thus, the frequency dependence of these gains will be distorted. It is, therefore, possible that one of the important consequences of self-absorption may be the shifting of the oscillation frequencies from the line centers. Fig. 1 shows the net gain for two overlapping lines, with the line center shifted (in this case pushed) by an amount $\delta\nu$. A similar effect resulting in pulling can occur if the neighboring resonant line exhibits gain rather than absorption.

The magnitude of these frequency shifts may be important for atmospheric transmission, and if so, experimental absorption measurements of transmission with low pressure probe lasers will not resolve the propagation question for radiation from high pressure devices. Furthermore, line selected devices employing an intracavity cell (e.g., with water vapor) will also have gain profiles with frequency distortion. For those lines predicted to have good atmospheric transmission (Table I), a small shift in frequency would probably not have serious consequences for atmospheric transmission, since absorption is primarily from wings of water vapor lines. However, transitions in bands greater than $6 \rightarrow 5$, which are now predicted to have bad atmospheric propagation characteristics, lie on the sharp edges of water vapor absorptions. Thus, a frequency shift for these lines (either by self-absorption in CO or by dispersive intracavity line selection) may result in favorable transmission for such lines.

The calculations which are in progress to include effects of self-absorption in the laser kinetics model will include predictions of line frequency shifts. Furthermore, calculations based on the McClatchey AFCRL model atmosphere will be undertaken to assess the sensitivity of anticipated line shifts on atmospheric propagation.

FIGURE CAPTION:

Figure 1: Frequency dependent gain for overlapping, collisionally broadened, near resonant lines. Transition with gain, centered at frequency ν_o, overlaps with absorption at $(\nu_o + \Delta\nu)$, with net gain reduced and shifted by $\delta\nu$.

TABLE I RESONANT TRANSITIONS FOR SELECTED CO LINES WITH GOOD ATMOSPHERIC TRANSMISSION

Laser Line	Frequency (cm^{-1})	Attenuation Range (km)*	Resonant Transitions	$\Delta\tilde{\nu}(cm^{-1})$
6 → 5 P(9)	1977.264	13.3	8 → 7 R(4)	.443
6 → 5 P(10)	1973.285	14.3	8 → 7 R(3)	-.111
			9 → 8 R(11)	-.095
			10 → 9 R(20)	-.018
5 → 4 P(9)	2003.154	18.5	7 → 6 R(4)	.101
			8 → 7 R(12)	.238
5 → 4 P(14)	1982.754	13.2	4 → 3 P(20)	-.011
			9 → 8 R(14)	.185
5 → 4 P(15)	1978.575	22.7	- -	-
5 → 4 P(16)	1974.362	15.4	7 → 6 P(3)	-.032
5 → 4 P(20)	1957.189	30.3	6 → 5 P(14)	.151
			9 → 8 R(6)	.145
4 → 3 P(7)	2037.113	11.5	- -	-
4 → 3 P(8)	2033.132	41.7	6 → 5 R(5)	.313
4 → 3 P(9)	2029.117	33.3	6 → 5 R(4)	-.244
			7 → 6 R(12)	-.311
4 → 3 P(10)	2025.068	13.3	- -	-
4 → 3 P(13)	2012.723	11.2	3 → 2 P(19)	-.101
4 → 3 P(15)	2004.326	22.7	6 → 5 P(2)	.165
4 → 3 P(20)	1982.765	13.0	5 → 4 P(14)	.011
			9 → 8 R(14)	.196
3 → 2 P(5)	2071.146	40.0	4 → 3 R(1)	-.250
			6 → 5 R(17)	-.333
3 → 2 P(8)	2059.200	10.0	5 → 4 R(5)	-.035
			6 → 5 R(13)	.018
3 → 2 P(10)	2051.066	16.1	- -	-
3 → 2 P(13)	2038.615	16.9	2 → 1 P(19)	.042
			7 → 6 R(15)	-.099
3 → 2 P(15)	2030.148	20.8	5 → 4 P(2)	-.149

*Calculations of D. K. Rice based on molecular absorption through horizontal path at sea level in a mid latitude Winter atmosphere. This model utilizes the McClatchey AFCRL major atmospheric constituent data covering wavelength from 1 μm to 20μm.

A 8

[1] M. L. Bhaumik, W. B. Lacina, and M. M. Mann, IEEE J. Quant. Elect. QE-8, 150 (1972).

[2] M. M. Mann, D. K. Rice, and R. G. Eguchi, Paper B. 7, presented at VIII Internat'l Quant. Elect. Conf., June 10-13, 1974, San Francisco.

[3] W. B. Lacina, M. M. Mann, and G. L. McAllister, IEEE J. Quant. Elect. QE-9, 588 (1973).

[4] W. B. Lacina and G. L. McAllister, "Scaling Generalizations for a CO Electric Laser," submitted to IEEE J. Quant. Elect.

[5] W. B. Lacina and G. L. McAllister, "Scaling of Parameters and Resonance Self-Absorption in CO Lasers," Northrop Report No. NRTC-74-48R, September, 1974.